Chapter 4
TWIN SLOT ANTENNA STRUCTURES

For the far infrared spectral region, there is an incentive for using planar antennas rather than bulky, expensive, metallic waveguide structures [1]. One such planar structure is the slot antenna [2], which in its simplest configuration is simply a narrow rectangular slot cut into a sheet of conductor (see Fig. 4.1(a)). The slot is narrow compared to a radiation wavelength, and its length is chosen to provide a resonant structure. By suspending a narrow microstrip line across the slot, as shown in Fig. 4.1(b), the slot can be coupled to a detector/feed network. A significant advantage of this structure is that the radiation can be incident on one side of the slot plane, while the feed lines and detectors are on the other side. The feed network is therefore shielded from the incident radiation. This can be significant for imaging or phased array applications where many feed lines are required [3].

A problem with planar antennas is their tendency to couple significant power into guided modes (also called surface waves) when the substrate is a significant fraction of a dielectric wavelength λ_d thick. Guided modes are a result of the substrate appearing as waveguide when the top and bottom surfaces are parallel [4]. Coupling into these surface waves can be avoided by making the substrate very thin, which cuts off most of the modes. At millimeter and submillimeter wave frequencies, however, electrically thin substrates are on the order of 50 μm or less, making fabrication extremely difficult. One successful planar antenna built for these frequencies was a log-periodic antenna fabricated on a 1 μm thick silicon oxynitride membrane [5]. Another way to avoid guided modes is to make the substrate appear infinitely thick. This is accomplished by placing a focusing lens on back of the substrate [6]. A third approach to reduce surface wave losses involves placement of a properly spaced pair of slots on a carefully chosen substrate. Such a twin slot antenna has been used as a component in a quasi-optical mixer operating at 100 to

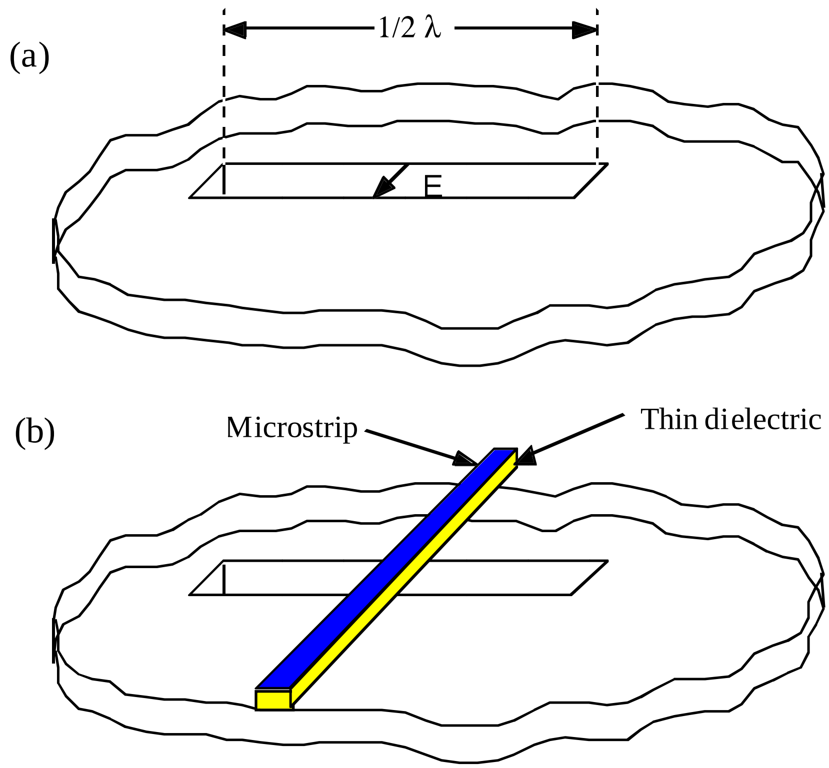

Fig. 4.1: The slot antenna. (a) The slot is one-half wavelength long, and the E-field is perpendicular to the long dimension of the slot. The ground plane is much larger than the slot, and is sandwiched by air in this simplest configuration. (b) The E-field in the slot couples to a microstrip line.

120 GHz [7]. Further improvement in the gain and the beam pattern can be achieved by placing the twin slot antenna structure on a selected stack of dielectrics [8]. The twin slot antenna on a dielectric stack is shown in Fig. 4.2. The feed network supported by a thin dielectric is shown raised from the slot groundplane surface for easier viewing. The twin slot antenna couples power into a microstrip feed line which consists of microstrip low-pass filters and a bismuth microbolometer detector. To test the theory, twin slot structures operating at 90.5 and 94 GHz are demonstrated.

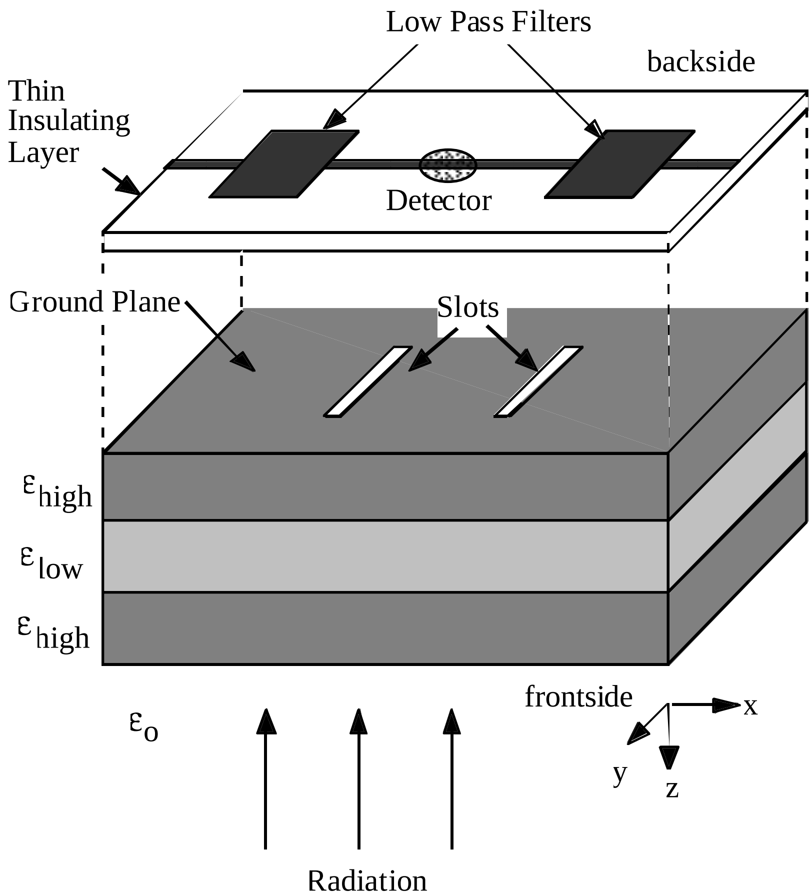

Fig. 4.2: Twin slot antenna on a dielectric stack, where each layer is 1/4 wavelength thick. The slots couple power into a microstrip line supported over the slots by a thin insulator. This power is dissipated in a detector, and is isolated from the rest of the feed network by low pass filters.

4.1 Theory

The theory underlying a twin slot antenna on a dielectric stack has been covered in extensive detail by Rogers *et al.* [[9,10]-[11]]. In this theory, it is much easier to treat the twin slot antenna structure as a source of radiation rather than as a receiver. By the electromagnetics rule of reciprocity, efficiencies and beam patterns will be the same for both source and receiver. Briefly, the total power emitted by a twin slot antenna consists of the power radiated through the dielectric (the "front side" of the structure), the power lost to surface waves, and the power radiated directly to air (the "backside" of the structure). For most efficient operation, power through the front side is desired maximum. To calculate radiated power, equivalent transmission line models of the dielectric stack are used, and each slot is modeled as a voltage source. To calculate power lost to surface waves, a reciprocity method described by Rutledge *et al.* is used [1]. In this section, the theory will be explained qualitatively.

Figure 4.3 shows the onset of guided modes as a function of substrate thickness for a slot antenna. Power lost to guided modes is desired minimum for an efficient planar antenna structure. The TM_o mode is seen to cut on almost immediately, whereas the TE_o mode cuts on at just past one-quarter wavelength λ_d. Surface wave losses are minimized, it turns out, by restricting the substrate thickness to odd multiples of 1/4 λ_d [12]. A dielectric of thickness 1/4 λ_d is the most efficient case, but power is still lost to the TM_o mode. Figure 4.4 illustrates a solution. If a pair of slots is placed one half a TM_o wavelength apart, and the slots

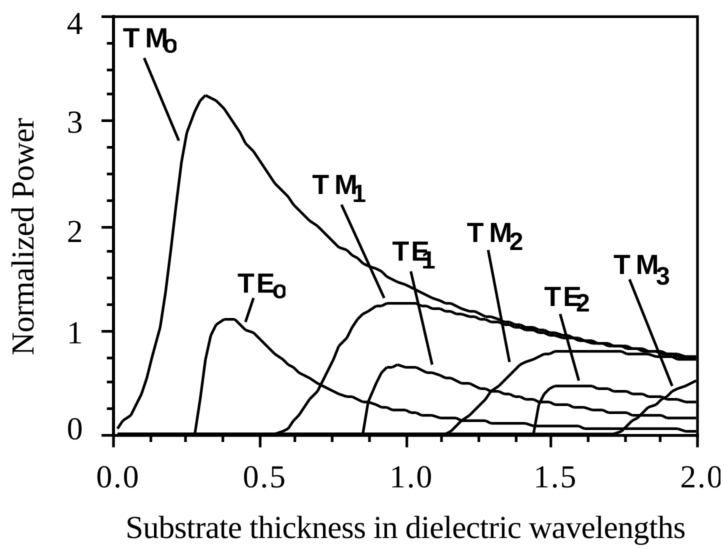

Fig. 4.3: Power distribution for the guided modes of a slot antenna as a function of substrate thickness. Adapted from [12].

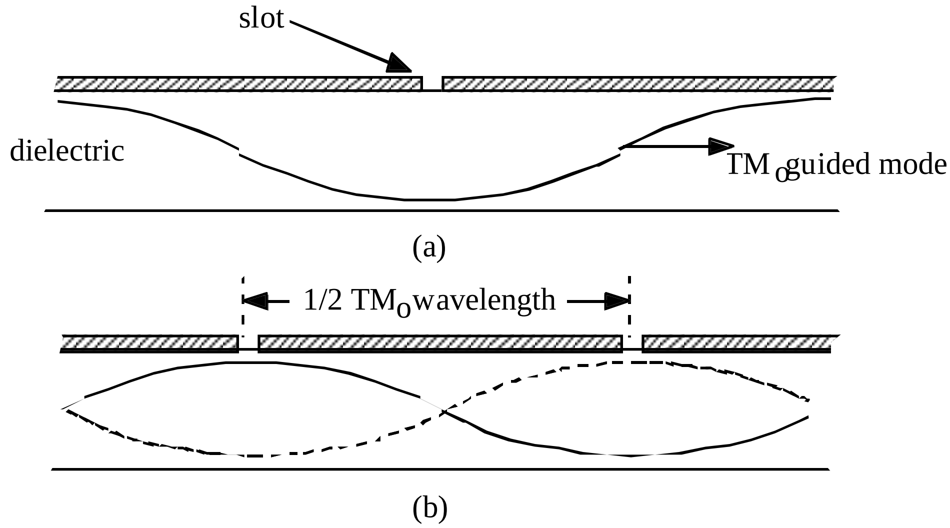

Fig. 4.4: Twin slots can be used to cancel the TM_o mode. (a) The single slot showing the TM_o mode. (b) TM_o modes from the two slots 1/2 TM_o wavelength apart will superimpose and cancel.

are driven in-phase, then the TM_o modes from each slot will superimpose and cancel [13]. Of course, the dimensions chosen are frequency dependent, so it is practically impossible to eliminate all of the surface waves this way.

Using twin slots on a 1/4 λ_d thick substrate minimizes power lost to surface waves. Now the power radiated through the backside must be minimized. Planar antennas placed on a dielectric substrate tend to radiate more power through the dielectric than directly into air [14]. Placing a slot antenna on a stack of dielectrics can further reduce radiation through the backside of the structure, and will also narrow the beamwidth of radiation through the frontside [9,15]. The concept is best understood by examining the transmission line model shown in Fig. 4.5. In this figure, the slot is represented by a voltage source. Maximum power is delivered into a minimum impedance load. The impedance Z_{in} looking into a line of impedance Z_o and terminated in a load impedance Z_L is given by the equation

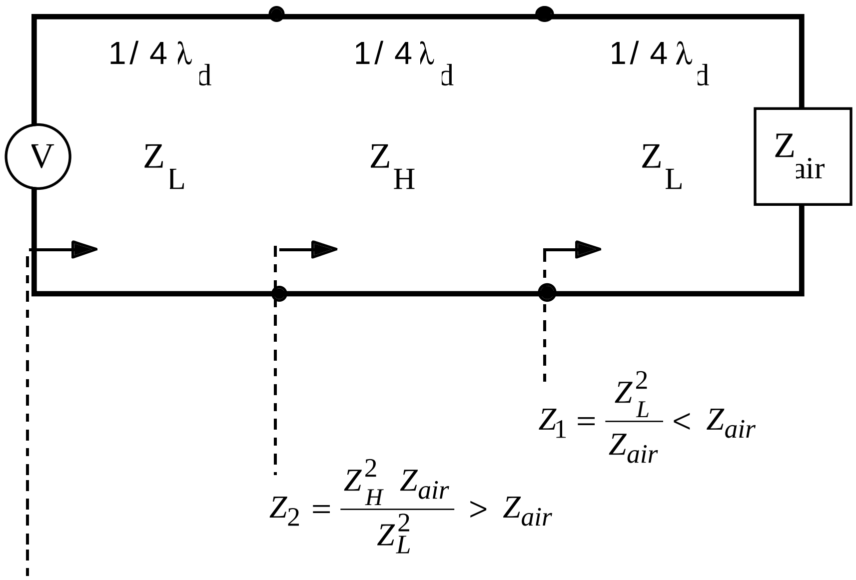

$$Z_1 = \frac{Z_L^2}{Z_{air}} < Z_{air}$$

$$Z_2 = \frac{Z_H^2\ Z_{air}}{Z_L^2} > Z_{air}$$

$$Z_3 = \frac{Z_L^4}{Z_H^2\ Z_{air}} < Z_1 < Z_{air}$$

Fig. 4.5: Transmission line model for a twin slot antenna on a stack of $\lambda_d/4$ thick dielectrics. The slots are modeled as a voltage source. A Z_L (low impedance)-Z_H (high impedance)-Z_L configuration terminated in the impedance of air has a lower impedance than a single layer of dielectric. Hence, more power will be radiated.

$$Z_{in} = Z_o \frac{Z_L \cos \beta L + j\, Z_o \sin \beta L}{Z_o \cos \beta L + j\, Z_L \sin \beta L} \tag{4.1}$$

where β is the phase constant, equal to $2\pi/\lambda_d$, and L is the length of the line. If each dielectric in the stack is chosen to be 1/4 λ_d thick, then the equation reduces to

$$Z_{in} = \frac{Z_o^2}{Z_L}\ . \tag{4.2}$$

This is an impedance inverter. The impedance looking into the first dielectric layer Z_1 is less than the impedance of air, since the line impedance Z_L is less than Z_{air}. Impedances looking into the second and third layers are shown in Fig. 4.5. The lower impedance seen looking into the third layer will result in more power radiated by the slots on a dielectric stack than for slots on a single dielectric. This low-high-low impedance structure corresponds to a high-low-high dielectric constant structure.

The dielectric substrate which supports the antenna also forms a waveguide structure which will cause undesirable loss of power to guided (or surface) waves. However, if the substrate consists of an odd number of 1/4 λ_d thick layers, alternating from high to low to high dielectric constant, it is possible to restrict the surface wave losses to one dominant mode, usually the TM_o mode [[16]]. If a pair of slots is placed one half a TM_o wavelength apart in the broadside direction, and the slots are driven in-phase, then the TM_o modes from each slot will superimpose and cancel [10]. Thus, the same dielectric stack which maximizes radiated power through the dielectric can also be used to suppress surface wave losses when used in conjunction with twin slots.

Another concern in the operation of a twin slot antenna is the coupling efficiency to the microstrip feed line/detector network. Rogers *et al.* [11,[17]] detail the analysis used to calculate the impedance of the twin slot structure as seen by the detector. It is shown that choice of feed line length between the slots, as well as other considerations, can have a strong influence on the coupling.

4.2 Fabrication

To test the theoretical models cited [9-11], we have investigated the performance of twin slot antennas operating on an ordinary glass slide, and operating on a fused quartz substrate. The slot dimensions and the fused quartz thickness were chosen based on operation at 94 GHz. An ordinary soda-lime microscope slide was first used to develop the process, and to provide a test case considerably removed from the design structure. Soda-lime glass has a fairly high loss tangent of ~ 0.023 and a high frequency dielectric constant ε_r = 6.7 [[18]]. Once the process was determined, the optimized test structure was fabricated on a 406 μm thick fused quartz substrate (1/4 λ_d at 94 GHz) supplied by Bond Optics. This quartz has a loss tangent of <0.0001 and ε_r = 3.8 [19].

Fabrication of the optimized structure started with a 2.5 cm x 2.5 cm square fused quartz substrate. The basic fabrication sequence is shown in Fig. 4.6. The ground plane was deposited on the substrate by thermal evaporation of ~300 Å of chromium for adhesion followed by ~6000 Å of gold (slightly more than two skin depths at 94 GHz), in a vacuum maintained under 10^{-5} torr. This was about the

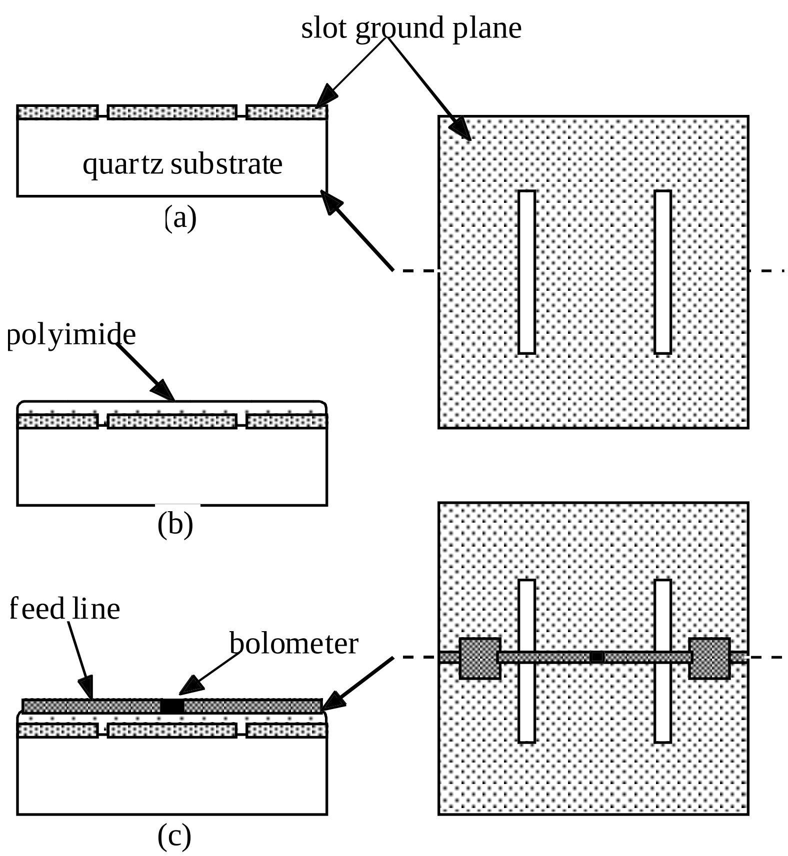

Fig. 4.6: Top views (right) and profiles (left) of the twin slot structure at various points in the basic fabrication sequence. (a) Slots are etched into a thick metal ground plane. (b) A thin layer of polyimide is applied and cured. (c) The feed line and microbolometer are fabricated using a photoresist bridge technique.

maximum thickness that was practical to achieve using this technique. Thickness was measured during the evaporation with a crystal thickness monitor. The slots were then chemically etched into the ground plane (see Fig. 4.6(a)). Following the etch, the slots were measured under a microscope. The slots were 950 μm apart, center to center, and each slot was 1170 μm long by 46 μm wide. Figure 4.7 shows the feed line and detector in the vicinity of the slots. Notice that the feed line between the slots has been lengthened; it does not go straight across. Impedance calculations [11] show the impedance of the slots as seen by the detector is maximum for feed line lengths a multiple of a microstrip guide wavelength λg apart.

The feed network is separated from the slot plane by a 2 μm thick polyimide layer (DuPont Pyralin PI-2556 polyimide) as shown in Fig. 4.6(b). A thorough cure step was required because the polyimide dissolves in photoresist developer when it is insufficiently cured. The temperature and duration of the cure also influences the dielectric constant and the loss tangent of the polyimide [20]. The cure step was carried out at 250 °C for a duration of 1.5 hours.

Fabrication of the bismuth microbolometer and the feed line (Fig. 4.6(c)) was accomplished using a bilayer photoresist bridge technique [21,22], which has been detailed in chapter 3.The transparency of the buffer layer using this method is quite important for aligning the feed network over the slots, and is one reason we chose this process instead of a bilayer process which uses aluminum as the separator [23].

The Bi microbolometer shown in Fig. 4.8 is approximately 1000Å thick, 3 μm long and 3 μm wide. The feed lines are 25 μm wide,with a 1000 Å thick layer of Ag topped by a 2000 Å thick layer of Bi, and finally a 2000 Å thick layer of Ag (the much higher conductivity of Ag essentially shorts the Bi in the feed line). Bi microbolometer resistance was measured to be about 80 Ω, and the microstrip impedance was calculated to be about 13-16 Ω based on empirical formulas [24-2526]. The series resistance of the microstrip line between the innermost filters for the $1\lambda_g$ feedline length case was measured as 18 Ω (~0.23 Ω/square). For the fused quartz structure, the room temperature microbolometer responsivity was measured to be about 7.2 V/W when biased at 0.1 V.

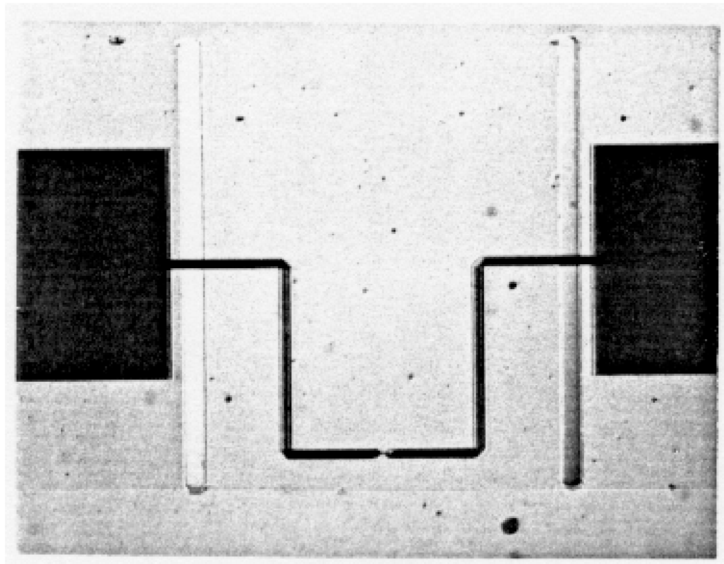

Fig. 4.7: The twin slot antenna shown with feed lines, detector, and low pass filters. Magnification is ~ 50X.

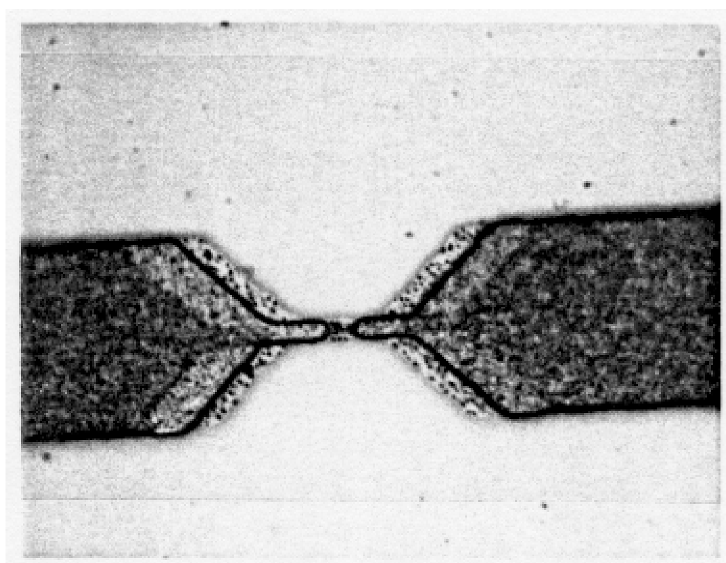

Fig. 4.8: Bismuth microbolometer at the narrow region between two microstrip feed lines.magnified ~1000x.

Placement of a quarter wavelength thick quartz layer one quarter of a wavelength above the substrate results in a "resonant" structure similar to those described in [15]. The quartz-air-quartz stack, corresponding to $\varepsilon_{high} = 3.8$ and $\varepsilon_{low} = 1.0$ in Fig. 4.2, was made by placing a 1/4 λ_d thick (406 μm) fused quartz chip over the substrate, using small spacers 860 μm thick placed at the corners of the chip.

Several details are different for the soda-lime glass structures. First, the soda lime glass was ~1170 μm thick, which is comparable to a dielectric wavelength thick. Second, the slots were etched into a 4000 Å thick copper ground plane, rather than a 6000 Å thick gold layer. And third, the bismuth microbolometers had a lower room temperature responsivity (magnitude about 4-5 V/W).

4.3 Measurement

Electrical connection was achieved by placing the chip on a small microwave laminate board, and connecting pads on the chip to copper pads on the board using silver paint. The chip was placed in a positioning mount with the twin slot antenna at the center, allowing the antenna to pivot in the E- and H-planes. The general measurement setup is shown in Fig. 4.9. A Hughes IMPATT W-band oscillator connected to a standard gain horn was placed approximately 36 cm from the antenna. Laser alignment was used to determine boresight and to align the chip plane parallel with the plane of the horn. The radiation was chopped at 200 Hz, and the signal was measured with a Stanford Research Systems SR530 lock-in amplifier. Measurements were taken at 4° increments in both E- and H-planes, and the detected signals ranged from 6 μV down to the background noise level of about 0.02 μV.

The power delivered to a receiver is given by Johnson [27],

$$P_r = \left(\frac{\lambda}{4\pi R}\right)^2 G_t\, G_r\, P_t \qquad (4.3)$$

where λ is the free-space wavelength of the radiation, R is the distance from the horn to the antenna (36 cm), G_t is the gain of the horn (24 dB), P_t is the transmitted

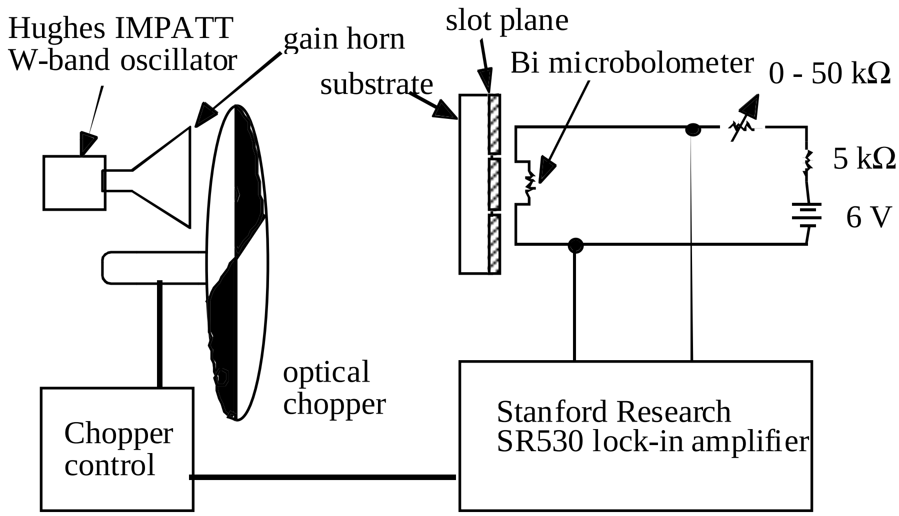

Fig. 4.9: The general setup used in range testing the twin slot antenna.

oscillator power measured at the horn input (4 mW), and G_r is the received gain at the detector. The power received at the detector is determined by taking the signal voltage at the detector V_{sig} and dividing by the detector responsivity **r**. Responsivities for the bolometers used in this study are listed in Table 4.1. The detected power will differ from the power received by the antenna because of i) coupling loss between the microstrip and the slots, ii) losses in the microstrip, and iii) impedance mismatch loss between the microstrip and the microbolometer. These terms are lumped into the receiver gain, giving

$$G_r = \left(\frac{4\pi R}{\lambda}\right)^2 \frac{V_{sig}}{G_t\, P_t\, \mathbf{r}} \quad . \tag{4.4}$$

Receiver gain beam patterns are plotted in Figs. 4.10-4.14 for cases of interest.

Substrate:	Soda Lime		Fused Quartz	
Feed line length (in wavelengths)	1	2	1	2
-r (V/W)	4.1	5.2	7.2	7.1

Table 4.1. Bismuth microbolometer responsivities.

In Fig. 4.10, the receiver gain beam patterns are compared for different feed line lengths on a soda lime substrate. These plots show that considerable loss may be attributed to the microstrip feed line; gain for a total feed line of $2\lambda_g$ length is about 6 dB lower than for a $1\lambda_g$ total length. This 6 dB difference was also observed for the twin slot antenna on a fused quartz substrate. Assuming bulk conductivity for a pure silver microstrip line, microstrip losses are calculated to be about 3 dB per λ_g [11]. However, using the measured sheet resistance for the line, microstrip losses increase to about 7 dB.

Although microstrip conductor loss appears to account for all of the loss observed, three other loss mechanisms may also contribute. First, because of the way the devices are fabricated, there is a significant length of feed line that has only Bi on the outer edges; this could contribute to rf loss. Second, there is dielectric loss in the thin polyimide layer, but we do not consider this to be significant. Third, there may be a difference in impedance mismatch loss between the two lines considered above. The impedance seen by the detector looking towards the slots is a function of feed line length. However, this impedance is calculated to be about the same for both the 1 λ_g and 2 λ_g cases [11].

There appears to be two sources of the jaggedness in these beam patterns. The first source is the effect of a finite ground plane. Radiation striking the edges of the ground plane excites currents in the plane which interfere with the wave directly incident on the slots, thus influencing the E-plane beam patterns. H-plane patterns are not disturbed. The second source of jaggedness is from surface waves. These waves may scatter off the edge of the slot ground plane, propagate along the substrate to the slots, and then interfere with the incident radiation. To a large extent, loss from surface waves can be reduced by placing ferrite-loaded absorber around the top periphery of the chip, which reduces the reflection of surface waves at the ground plane discontinuity. Figures 4.11(a) and 4.11(b) show the effect of adding absorber to a multilayer stack twin slot antenna operating at 90.5 GHz. The stack consists of 1/4 λ_d thicknesses of quartz, air, and quartz corresponding to relative dielectric constants of 3.8, 1, and 3.8. Smoothing of the E-plane beam pattern is quite apparent, but the H-plane is only slightly effected.

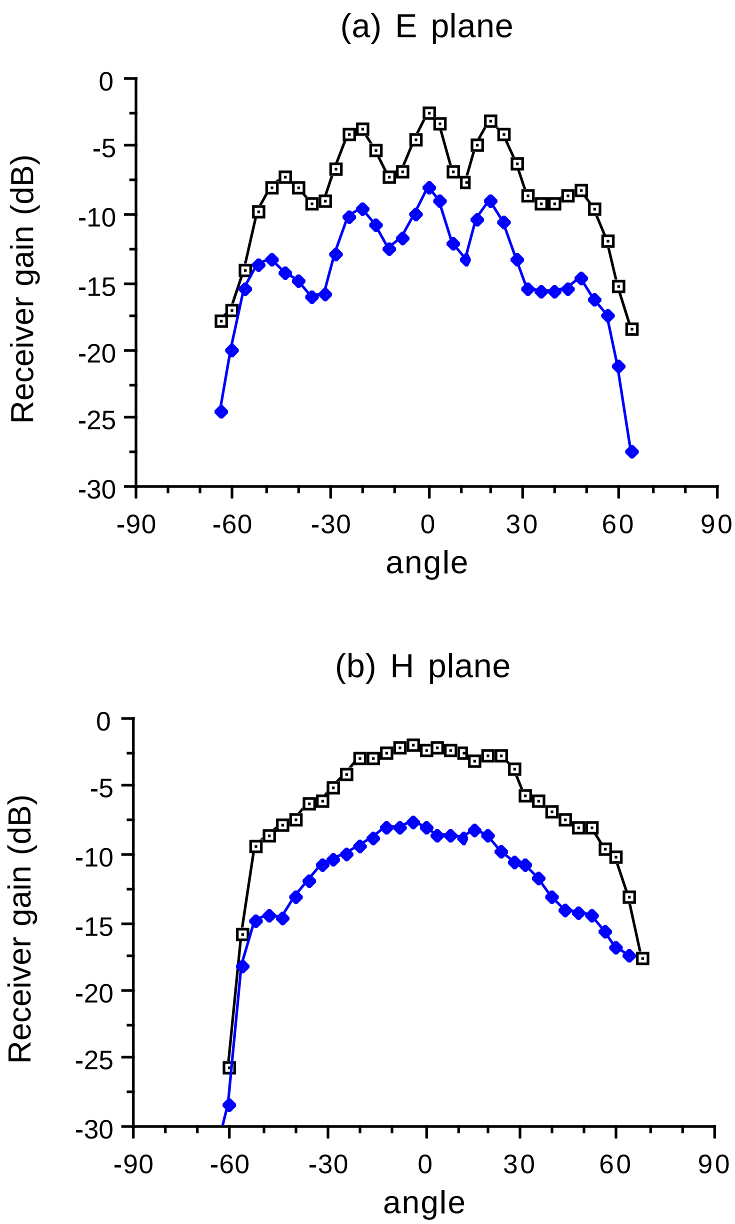

Fig. 4.10: The receiver beam patterns are compared for feed line lengths of $1\lambda_g$ and $2\lambda_g$. The $1\lambda_g$ patterns are topmost with light squares, and the $2\lambda_g$ patterns have the black dots. (a) and (b) show the E and H plane patterns for a soda lime (glass) substrate operating at 90.5 GHz.

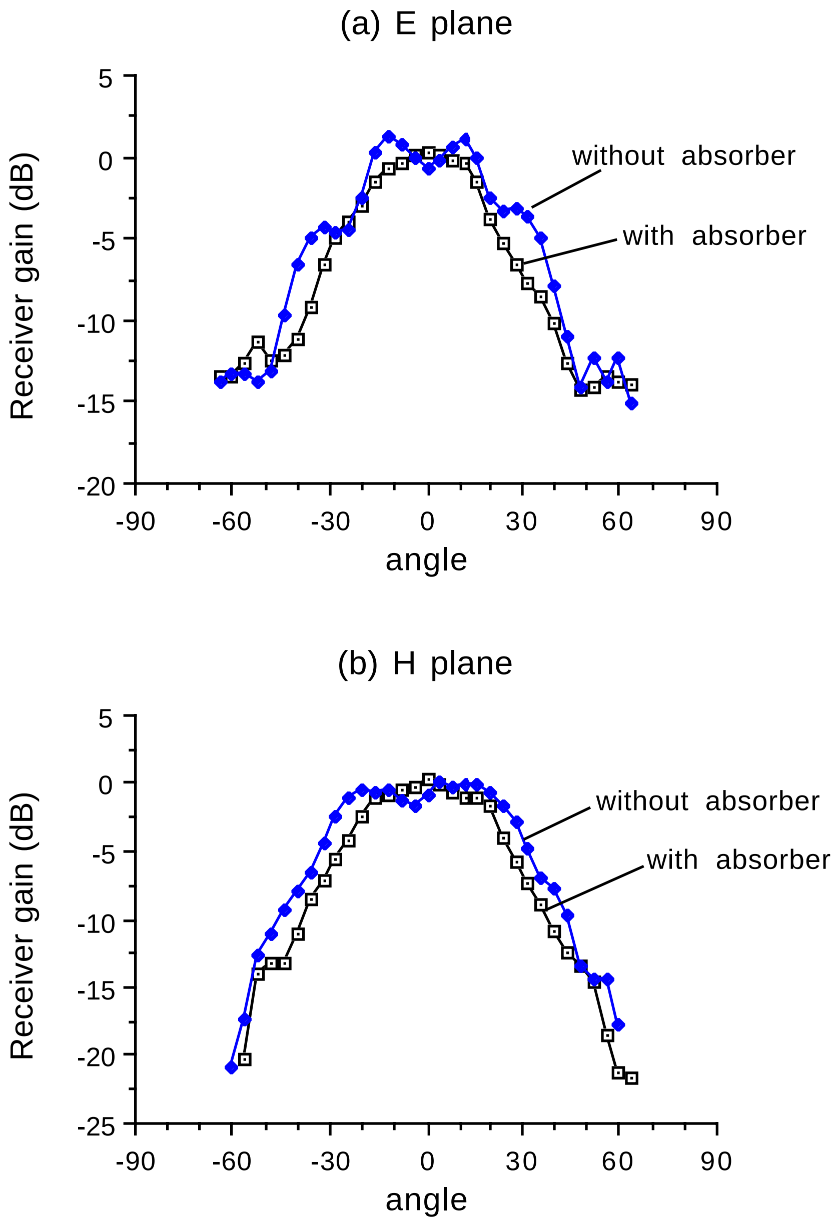

Fig. 4.11: The effect of using ferrite-loaded absorber around the edge of the slot ground plane is shown in the beam patterns for a fused quartz multilayer stack at 90.5 GHz.

Figure 4.12 shows the receiver gain beam patterns for the single fused quartz substrate operating at 90.5 GHz compared with theory. Ferrite-loaded absorber has been placed around the top periphery of the chip to reduce surface wave effects. There is considerable asymmetry between the E- and H-planes, which would be undesirable for optical system feeds. The shape of the measured E-plane agrees reasonably well with the theoretical model. We conjecture that the slightly jagged peaks are associated with finite ground plane effects, and with interference from surface waves reflecting back from the edges of the ground plane. The shape of the H-plane beam pattern shows only rough agreement with theory. We again assume that this is primarily a result of guided waves reflecting off the ground plane edge. There may also have been interference from adjacent pairs of slots, which were 0.5 cm distant from the center element in the H-plane. The sudden drop for the H-plane pattern at -56° is due to the shadowing from the antenna positioner mount.

Figures 4.13 and 4.14 show beam patterns for the multilayer stack at 90.5 and 94 GHz, respectively. The stack consists of a fused quartz substrate, an air gap, and a fused quartz cover layer (each of these layers nominally 1/4 λ_d thick). A ferrite-loaded absorber was once again used. Although the antenna is designed for 94 GHz, the air gap was slightly thicker (~864 μm) than the 1/4 λ_d design thickness (787 μm). Experimentally, the narrowest beam pattern was found at 90.5 GHz, which was also predicted by theory. In both figures, the theoretical beam pattern shapes are approximately matched by experiment. The boresight gain does not change noticeably between 94 and 90.5 GHz. This could be quite convenient in lens-coupled receivers where the beam pattern is not critical, but where the gain is desired constant over some appreciable bandwidth.

Comparing the single and multilayer 90.5 GHz results of Figs. 4.12 and 4.13, the theory predicts a boresight gain about 6 dB higher for the multilayer case. This increase is indeed observed since the boresight detector signal increases from 1 μV to 4 μV when the additional layer and air gap are added. It is also observed that compared to the single layer case, the measured and calculated patterns for the multilayer case.are narrowed.

The theory predicts at least a 10 dB higher receiver gain than is achieved by any of the experimental cases. However, the theory does not consider losses in the

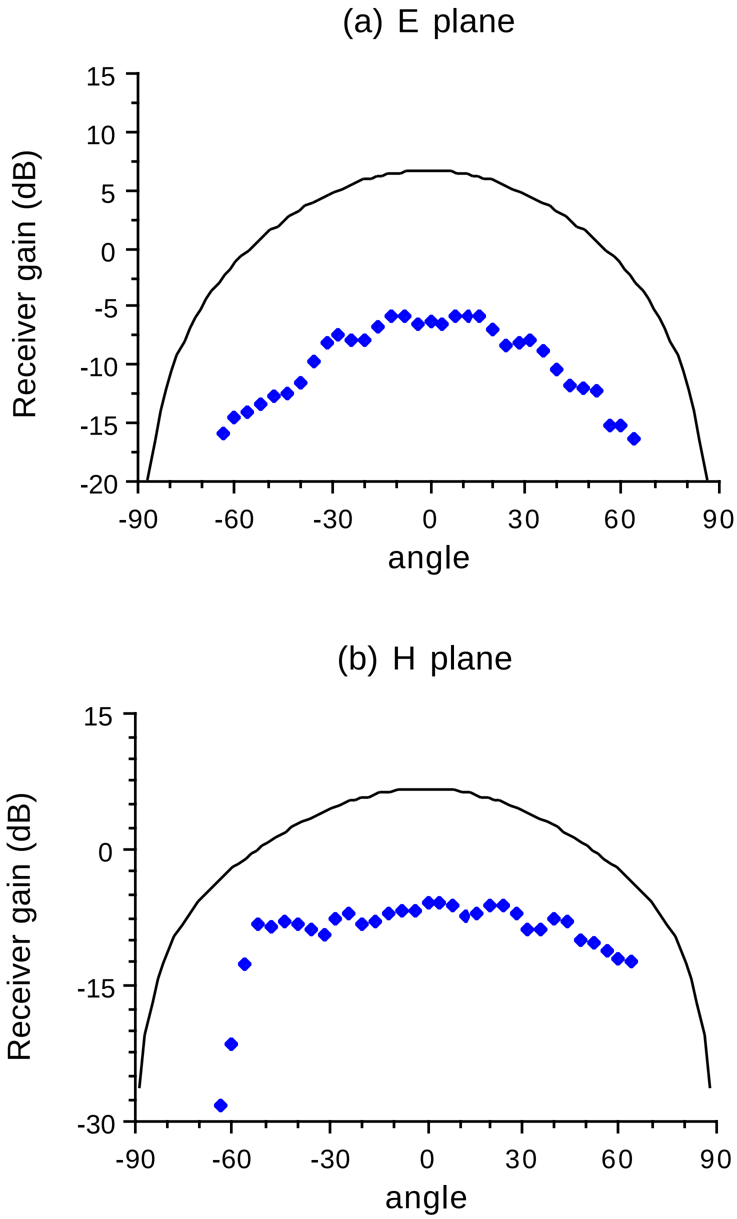

Fig. 4.12: (a) E-plane and (b) H-plane beam patterns for a twin slot antenna on a single 1/4 λ_d thick fused quartz substrate for 90.5 GHz radiation. Theory (solid line) is compared with experiment.

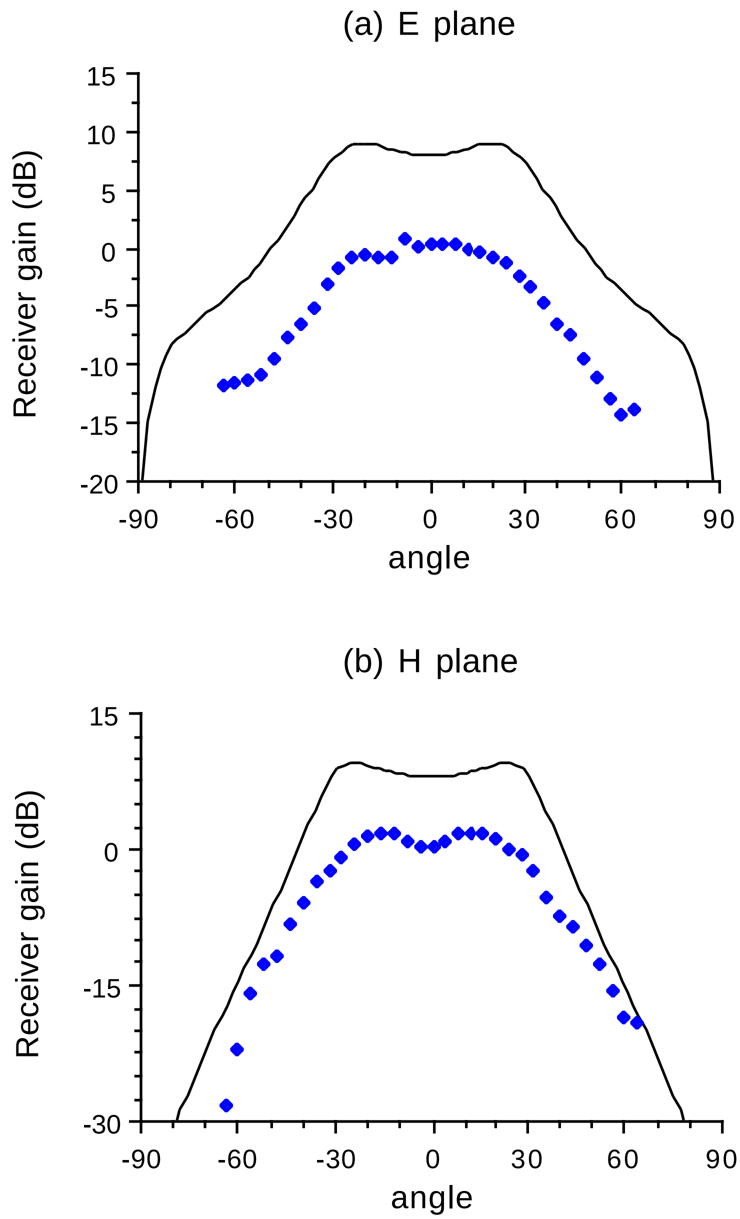

Fig. 4.13: (a) E-plane and (b) H-plane beam patterns for a twin slot antenna on a multilayer stack (dielectric constants 3.8,1, and 3.8) for 94 GHz radiation. Theory (solid line) is compared with experiment.

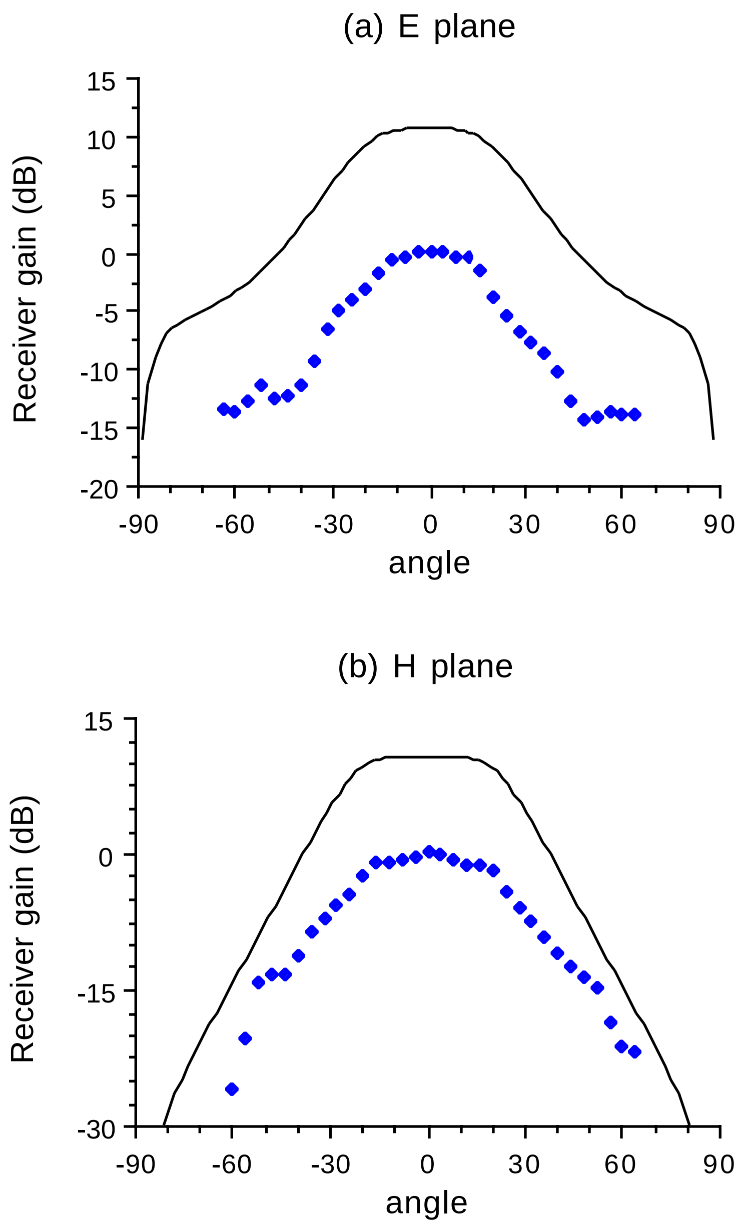

Fig. 4.14: (a) E-plane and (b) H-plane beam patterns for a twin slot antenna on a multilayer stack (dielectric constants 3.8,1, and 3.8) for 90.5 GHz radiation. Theory (solid line) is compared with experiment.

feedline, nor does it consider mismatch losses between the detector and the feed line. Based on the measurements shown in Fig. 4.10, 6 dB of feedline loss is expected. Another 3 dB mismatch loss is expected between the detector (80 Ω resistance) and the microstrip feedline (13-16 Ω impedance). Another possible loss mechanism is rf power loss through the low pass filters, which may not have a low enough impedance compared to the microstrip line.

4.4 Conclusions

A planar receiver has been demonstrated which consists of a twin slot antenna on a dielectric stack and a microbolometer detector. There was significant loss found in the microstrip feed line, and in surface waves radiating at the slot ground plane edge. The judicious use of ferrite-loaded absorber placed along the edges of the ground plane smoothed the beam pattern by reducing surface wave effects. As expected from theory, a higher gain beam pattern was obtained when a quartz-air-quartz dielectric stack was used.

Both theoretical models and experimental measurements show that although all the dimensions used for this antenna structure (i.e. the dielectric layer thicknesses, slot length, slot separation, and microstrip feed network length) are referenced to a single design frequency, the operating bandwidth is reasonably broad, without dramatic changes in either gain or pattern over at least a 5% variation in frequency.

There are a number of losses in the present system that could be reduced, providing further improvement in the performance of the dielectric stack/twin-slot antenna. The feed line conductor loss may be reduced by using a thicker polyimide support layer. This raises the characteristic impedance which would also reduce the mismatch loss. Dielectric loss in the polyimide could be reduced by finding the optimum curing conditions to minimize polyimide loss tangent [20]. The finite ground plane effects may be reduced by making the ground plane larger. Finally, mismatch losses between the microbolometer and the microstrip can be improved by using a thicker (lower resistance) layer of bismuth. However, Bi microbolometer responsivity will decrease for thicker layers. Research is underway to address these issues [[28]].

References:

[1]. D.B. Rutledge, D.P. Neikirk, and D.P. Kasilingam, "Integrated Circuit Antennas," Infrared and Millimeter Waves, Vol. 10, Academic Press, pp. 1-90, 1983.

[2]. J. Blass, "Slot Antennas," in Antenna Engineering Handbook, R.C. Johnson and H. Jasik, eds., McGraw-Hill, 1984.

[3]. D.M Pozar and D.H. Schaubert, "Comparison of Architectures for Monolithic Phased Array Antennas," *Microwave Journal*, pp. 93-104, Mar 1986.

[4]. B. Roudot, J. Mosig, and F. Gardiol, "Surface Wave Effects on Microstrip Antenna Radiation," *Microwave Journal*, pp. 201-211, Mar 1988.

[5]. G.M. Rebeiz, W. G. Regehr, D.B. Rutledge, R.L. Savage, and N.C. Luhmann, Jr., "Submillimeter-Wave Antennas on Thin Membranes," *Int. J. Infrared and Millimeter Waves,* Vol. 8, No. 10, pp. 1249-1255, Oct. 1987.

[6]. D.P. Neikirk, D.B. Rutledge, M.S. Muha, H. Park, and C.X. Yu, "Progress in millimeter-wave integrated circuit imaging arrays," *Proc. SPIE*, 317, p. 206, 1981.

[7]. A.R. Kerr, P.H. Siegel, and R.J. Mattauch, "A simple quasi-optical mixer for 100-120 GHz," in *1977 IEEE MTT-S Int. Microwave Symposium Dig.*, pp. 96-98.

[8]. S.M. Wentworth, R.L. Rogers, J.G. Heston, D.P. Neikirk, and T. Itoh, "Millimeter Wave Twin Slot Antennas on Layered Substrates," *Int. J. Infrared and Millimeter Waves,* Vol. 11, No. 2, pp. 111-131, Feb. 1990.

[9]. R.L. Rogers and D.P. Neikirk, "Radiation Properties of Slot and Dipole Elements on Layered Substrates," *Int. J. Infrared and Millimeter Waves*, Vol 10, No. 6, pp. 697-728, 1989.

[10]. R.L. Rogers and D.P. Neikirk, "Use of Broadside Twin Element Antennas to Increase Efficiency on Electrically Thick Dielectric Substrates," *Int. J. Infrared and Millimeter Waves,* Vol. 9, No. 11, pp. 949-969, 1988.

[11]. R.L. Rogers, S.M. Wentworth, D.P. Neikirk, and T. Itoh, "A Twin Slot Antenna on a Layered Substrate Coupled to a Microstrip Feed Line," to be published in *Int. J. Infrared and Millimeter Waves*.

[12]. R. L. Rogers, "A Study of Slot and Dipole Antennas on Layered Electrically Thick Dielectric Substrates for Far Infrared and Millimeter Wave Imaging Arrays," Ph.D. thesis, The University of Texas at Austin, 1989.

[13]. D.B. Rutledge, D.P. Neikirk, and D.P. Kasilingam, "Integrated Circuit Antennas," Infrared and Millimeter Waves, Vol. 10, Academic Press, pp.1-90, 1983.

[14]. N.G. Alexopoulos, P.B. Katehi, and D.B. Rutledge, "Substrate Optimization for Integrated Circuit Antennas," *IEEE Trans. MTT*, Vol. 31, No. 7, pp. 550-557, 1983.

[15]. N.G. Alexopoulos and D.R. Jackson, "Fundamental Superstrate Effects on Printed Circuit Antennas," *IEEE Trans. Antennas and Propagation,* Vol. AP-32, No. 8, pp. 807-816, Aug. 1984.

[16]. R.L. Rogers, D.P. Neikirk, H. Ling, and T. Itoh, "Antennas on Layered Substrates," *13th Annual Conf. on Infrared and Millimeter Waves*, pp. 33-34, Dec. 1988.

[17]. R.L. Rogers, D.P. Neikirk, and T. Itoh, "Impedance Measurements and Calculations of a Microstrip-fed Slot Antenna on a Multilayered Electrically Thick Dielectric Substrate," *19th European Microwave Conference*, Sept. 4-7, 1989, pp. 167-171.

[18]. J.R. Birch, R.J. Cook, A.F. Harding, R.G. Jones, and G.D. Price, "The optical constants of ordinary glass from 0.29 to 4000 cm^{-1}," *J. Phys. D: Appl. Phys.*, Vol. 8, pp. 1353-1358, 1975.

[19]. K.H. Breeden and J.B. Langley, "Fabry-Perot Cavity for Dielectric Measurements," *Rev. Sci. Instrum.*, Vol. 40, No. 9, pp. 1162-1163, Sept. 1969.

[20]. G. Samuelson, "Polyimide for Multilevel Very Large-Scale Integration (VLSI)," in Polymer Materials for Electronic Applications, E.E. Feit and C.W. Wilkins, Jr., Eds., pp. 93-105,1982.

[21]. D.P. Neikirk, W.W. Lam, and D.B. Rutledge, "Far-Infrared Microbolometer Detectors," *Int. J. Infrared and Millimeter Waves*, Vol. 5, No. 3, pp. 245-278, 1984.

[22]. D. M. Dobkin and B. D. Cantos, "Plasma Formation of Buffer Layers for Multilayer Resist Structures," *IEEE Electron Device Lett.*, Vol. EDL-2, No. 9, pp. 222-224, Sept. 1981.

[23]. K. Grebe, I. Ames, and A. Ginzberg, "Masking of Deposited Thin Films by Means of an Aluminum-Photoresist Composite," *J. Vac. Sci. Technol.*, Vol. 11, pp. 458, Jan/Feb 1974.

24. T.C. Edwards, Foundations for Microstrip Circuit Design, Wiley and Sons, New York, pp. 44-47, 1981.

25. K.C. Gupta, R. Garg, I.J. Bahl, Microstrip Lines and Slotlines, Artech House, Inc., p.11, 1979.

26. I. Bahl and P. Bhartia, Microwave Solid State Circuit Design, Wiley and Sons, New York, p. 18, 1988.

27. R.C. Johnson and H. Jasik, Antenna Engineering Handbook, McGraw-Hill, pp. 1-12,13, 1984.

28. J.G. Heston, S.M. Wentworth, R.L. Rogers, D.P. Neikirk, and T. Itoh, “MM Wave/FIR Twin Slot Antenna Structures,” to be presented at the *IEEE AP-S International Symposium and URSI Radio Science Meeting*, Dallas, May 7-11, 1990.